Pose-invariant 3D Proximal Femur Estimation through Bi-Planar Image Segmentation with Hierarchical Higher-Order Graph-based Priors

Chaohui Wang[1,2] Haithem Boussaid[1,2] Loic Simon[1] Jean-Yves Lazennec[3] Nikos Paragios[1,2]

[1]Laboratoire MAS, Ecole Centrale de Paris, France
[2]Equipe GALEN, INRIA Saclay - Île de France, Orsay, France
[3]Centre Hospitalier Universitaire Pitié Salpêtrière, Paris, France

Introduction

- **Problem statement:**
  3D Proximal Femur modeling from low-dose bi-planar X-Ray images $\Leftarrow$ important diagnostic interest in *Total Hip Replacement*.
- **Contributions:**
  - Non-uniform hierarchical decomposition of the shape prior of increasing clinical-relevant precision.
  - Graphical-model representation of the femur involving third-order and fourth-order priors.
    - Similarity and mirror-symmetry invariant.
    - Providing means of measuring regional and boundary supports in the bi-planar views.
    - Can be learned from a small number of training examples.
  - A dual-decomposition optimization approach for efficient inference of the 3D femur configuration from bi-planar views.

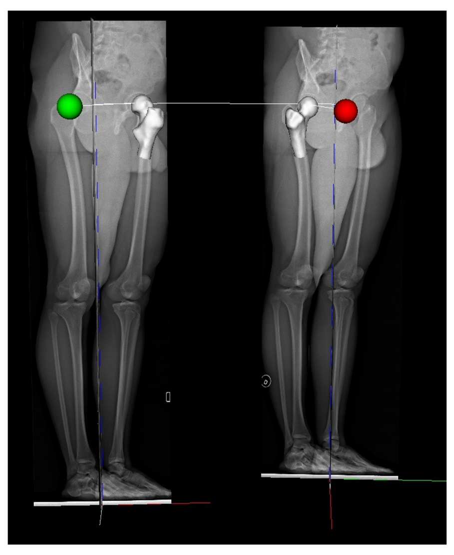

Hierarchical Multi-Resolution Probabilistic Modeling

- **Mesh sub-sampling** formulated as clustering achieved through curvature driven unsupervised clustering acting on the geodesic distances between vertices.

$$\mathcal{V}_{m+1} = \underset{\mathcal{V}\subset\mathcal{V}_m}{\operatorname{argmin}} \left[\sum_{v\in\mathcal{V}_m} \min_{\hat{v}\in\mathcal{V}} d(v,\hat{v}) + \alpha \sum_{\hat{v}\in\mathcal{V}} \exp(-\operatorname{curv}(\hat{v})) \right] \quad (1)$$

  - $d(v,\hat{v})$: the geodesic distance between v and $\hat{v}$ on $\mathcal{M}_0$,
  - $\operatorname{curv}(\hat{v})$: the curvature at $\hat{v}$ on $\mathcal{M}_0$.
- **Level of detail selection:**
  - Vertices are organized in a tree structure.
  - Starting from the coarsest resolution, regions are selected to be refined iteratively until reaching the required accuracy for every part.
    $\Rightarrow$**Vertices** $\mathcal{V}_{\mathbf{MR}}$
- **Connectivity computation**
  - **Edges** $\mathcal{E}_{\mathbf{MR}}$ based on Delaunay triangulation of $\mathcal{V}_{\mathbf{MR}}$ associated to the geodesic distance.
  - **Faces** $\mathcal{F}_{\mathbf{MR}}$ computed by searching for minimal cycles in the edge list.

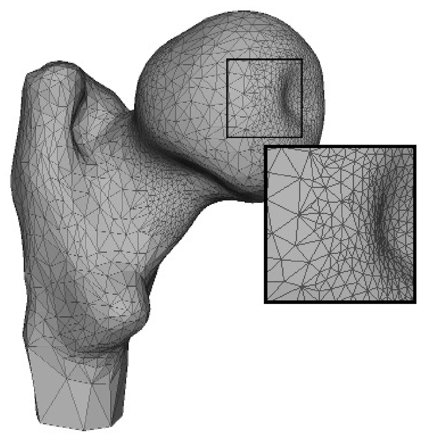

Figure: Multi-resolution surface Model

- **Probabilistic shape modeling**

$$p(\mathbf{u}) \propto \prod_{c\in\mathcal{T}} \psi_c(\hat{\mathbf{d}}_c(\mathbf{u}_c)) \cdot \prod_{q\in\mathcal{Q}} \psi_q(\mathbf{u}_q) \quad (2)$$

  - **Pose-invariant prior:**
    - Based on the relative Euclidean distance $\hat{d}_{ij} = d_{ij}/\sum_{(i,j)\in\mathcal{P}_c} d_{ij}$ for each pair of points $(i,j)\in\mathcal{P}_c$ in a triplet c of vertices.
    - The distribution $\psi_c(\hat{\mathbf{d}}_c)$ of $\hat{\mathbf{d}}_c$ is learned from the training data, using Gaussian Mixture Models (GMMs).
  - **Smoothness potential function:**
    Encoding constraints on the change of the normal directions, for each quadruplet q of vertices corresponding to a pair of adjacent facets:

$$\psi_q(\mathbf{u}_q) = \exp\{-(1 - <\vec{n}_q^{(1)}(\mathbf{u}_q), \vec{n}_q^{(2)}(\mathbf{u}_q)>)/\beta\} \quad (3)$$

Probabilistic 3D Surface Estimation Framework

- **Posterior probability maximization:**

$$p(\mathbf{u}|\mathbf{I},\mathbf{\Pi}) = \frac{p(\mathbf{u},\mathbf{I},\mathbf{\Pi})}{p(\mathbf{I},\mathbf{\Pi})} \propto p(\mathbf{u},\mathbf{I},\mathbf{\Pi}) = p(\mathbf{I}|\mathbf{u},\mathbf{\Pi})p(\mathbf{u})p(\mathbf{\Pi}) \propto p(\mathbf{I}|\mathbf{u},\mathbf{\Pi})p(\mathbf{u}) \quad (4)$$

$$E(\mathbf{u}) = -\log p(\mathbf{u}|\mathbf{I},\mathbf{\Pi}) + \text{constant}$$

- **Higher-order MRF formulation:**

$$E(\mathbf{u}) = \sum_{f\in\mathcal{F}} H_f^R(\mathbf{u}_f) + \sum_{q\in\mathcal{Q}} (H_q^B(\mathbf{u}_q) + H_q^P(\mathbf{u}_q)) + \sum_{c\in\mathcal{T}} H_c^P(\mathbf{u}_c) \quad (5)$$

  - $H_f^R(\mathbf{u}_f)$: regional-term potentials.
  - $H_q^B(\mathbf{u}_q)$: boundary-term potentials.
  - $H_c^P(\mathbf{u}_c)$ and H_q^P: model prior potentials.
- **MRF inference through dual-decomposition:**
  - Decompose the original graph into a series of factor trees.
  - Solve factor trees using max-product belief propagation.
  - Maximize lower bound using a projected subgradient method.

Observation Model

$$p(\mathbf{I}|\mathbf{u},\mathbf{\Pi}) = \prod_{k\in\mathcal{K}} p(I_k|\mathbf{u},\Pi_k) \quad (6)$$

- $\mathbf{I} = (I_k)_{k\in\mathcal{K}}$ ($\mathcal{K} = \{1,\ldots,K\}$, $K=2$ for the case of bi-planar views): K observed images captured from different viewpoints with the corresponding projection matrices $\mathbf{\Pi} = (\Pi_k)_{k\in\mathcal{K}}$.

$$p(I_k|\mathbf{u},\Pi_k) \propto \exp\{-\frac{\lambda E_k^{\mathrm{R}}(I_k,\mathbf{u},\Pi_k) + (1-\lambda)E_k^{\mathrm{B}}(I_k,\mathbf{u},\Pi_k)}{T_k}\} \quad (7)$$

T_k: temperature, $0<\lambda<1$: a balancing weight coefficient.

- **Regional term**

$$E_k^{\mathrm{R}}(I_k,\mathbf{u},\Pi_k) = \sum_{f\in\mathcal{F}} \delta_f(\mathbf{u}_f,\Pi_k) \cdot \iint_{\Omega(\mathbf{u}_f,\Pi_k)} \log\frac{p_{bg}(I(x,y))}{p_{fg}(I(x,y))} dxdy \quad (8)$$

  - $\mathbf{u}_f$: 3D coordinates of the vertices of a facet f,
  - $\delta_f(\mathbf{u}_f,\Pi_k)$: front-facing facet indicator function,
  - $\Omega_f(\mathbf{u}_f,\Pi_k)$: 2D region corresponding to the projection of f,
  - p_{fg} and p_{bg}: distributions of the intensity for the regions of the femur and the background.
- **Boundary term**

$$E_k^{\mathrm{B}}(I_k,\mathbf{u},\Pi_k) = \sum_{q\in\mathcal{Q}} \delta_q(\mathbf{u}_q,\Pi_k) \cdot \int_{\Gamma(\mathbf{u}_q,\Pi_k)} < \nabla I_k(x,y), \overrightarrow{n(x,y)} > ds \quad (9)$$

  - $\Gamma(\mathbf{u}_q,\Pi_k)$: projection of the edge shared by the two adjacent facets,
  - $\overrightarrow{n(x,y)}$: outward-pointing unit normal of $\Gamma(\mathbf{u}_q,\Pi_k)$, $\nabla I_k(x,y) = (\frac{\partial I_k(x,y)}{\partial x}, \frac{\partial I_k(x,y)}{\partial y})$: gradient of the intensity at (x,y).

Experimental Validation

- Validation using both dry femurs and real clinical data.
- Comparaison with the gold standard CT method, through *Point-to-surface distance* and *DICE coefficient*.

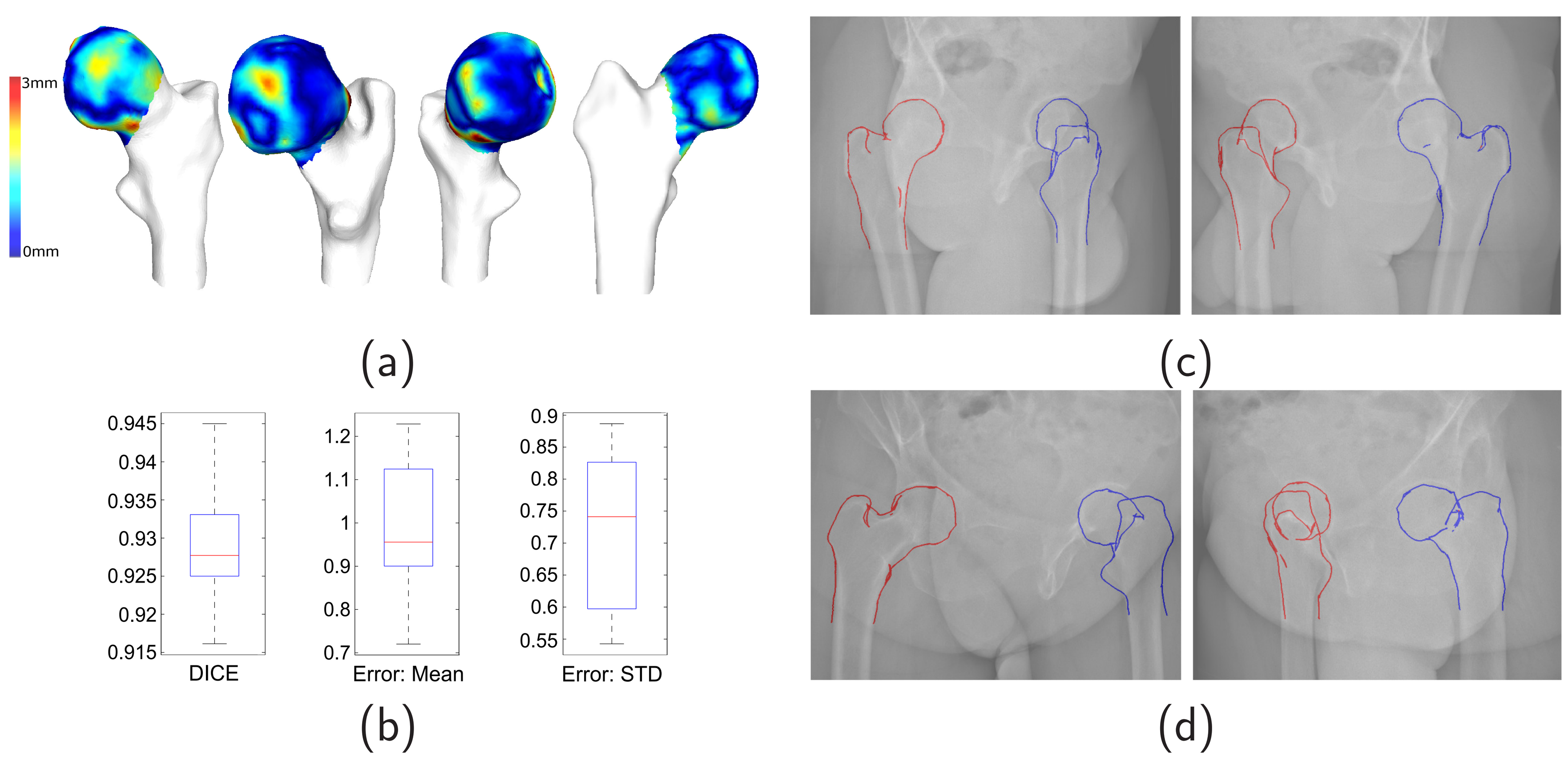

Figure: (a) Four 3D surface reconstruction results with point-to-surface errors on femoral head. (b) Boxplots on the DICE, the mean and STD of the point-to-surface errors (mm). (c) and (d) Projection results on in vivo data.

Future Work

- Introducing a joint model that couples femur with the hipbone socket.
- Combining anatomical landmarks with the existing formulation.
- Application to other clinical settings.

This work is supported by the European Research Council Starting Grant DIOCLES (ERC-STG-259112) and the MEDICEN Competitive Cluster sterEOS+ grant.

mailto: {chaohui.wang, haithem.boussaid}@ecp.fr